Direct 3-D morphological measurements of silicone rubber impression using micro-focus X-ray CT

Masayuki KAMEGAWA[1,2], Masayuki NAKAMURA[1,3,4], Yu FUKUI[4], Sadami TSUTSUMI[5] and Masaki HOJO[6]

[1]Department of Medical Simulation Engineering, Research Center for Nano Medical Engineering, Institute for Frontier Medical Sciences, Kyoto University, 53 Kawara-cho Shogoin, Sakyo-ku, Kyoto 606-8507, Japan
[2]Non-Destructive Inspection Business Unit, Analytical & Measuring Instruments Division, Shimadzu Corporation, 1 Nishinokyo-Kuwabaracho, Nakagyo-ku, Kyoto 604-8511, Japan
[3]Institute for Frontier Oral Science, Kanagawa Dental College, 82 Inaoka-cho, Yokosuka, Kanagawa 238-8580, Japan
[4]Ichiyoshi Dental Care Clinic, KTS-4F, 11-30 Higashinakano-cho, Akashi, Hyogo, Japan
[5]School of Dentistry, Nihon University, 1-8-13 Surugadai, Kanda, Chiyoda-ku, Tokyo 101-8310, Japan
[6]Department of Mechanical Engineering and Science, Kyoto University, Yoshida-honmachi, Sakyo-ku, Kyoto 606-8501, Japan
Corresponding author, Masayuki KAMEGAWA; E-mail: kamegawa@shimadzu.co.jp

Three-dimensional computer models of dental arches play a significant role in prosthetic dentistry. The microfocus X-ray CT scanner has the advantage of capturing precise 3D shapes of deep fossa, and we propose a new method of measuring the three-dimensional morphology of a dental impression directly, which will eliminate the conversion process to dental casts.

Measurement precision and accuracy were evaluated using a standard gage comprised of steel balls which simulate the dental arch. Measurement accuracy, standard deviation of distance distribution of superimposed models, was determined as ±0.050 mm in comparison with a CAD model. Impressions and casts of an actual dental arch were scanned by microfocus X-ray CT and three-dimensional models were compared. The impression model had finer morphology, especially around the cervical margins of teeth.

Within the limitations of the current study, direct three-dimensional impression modeling was successfully demonstrated using microfocus X-ray CT.

INTRODUCTION

Three-dimensional (3D) computer models of dental arches play a significant role in orthodontics and prosthodontics. Optical scanners that generate 3D computer models of dental casts have been proven to provide sufficient system accuracy for clinical application[1,2,3], therefore, optical scanners were used alongside computer-aided design and manufacturing (CAD/CAM) systems to produce dental restorations[4]. In particular, when scanning single teeth, the accuracy is satisfactory for practical use[5]; however, dental casts have a complex shape with an undercut, and an optical scanner is required to measure from a number of directions to minimize blind areas that need to be synthesized. Nevertheless, this technique does not provide adequate accuracy for pits and fossae, especially around the cervical margins of teeth. This deficiency becomes more acute when measuring complete dental arches *versus* individual, separate teeth.

Microfocus X-ray CT has been developed for industrial use[6] and has been investigated for dental applications using its features of nondestructive internal structure inspection[7,8]. In dental implant research, microfocus X-ray CT has been used to evaluate bone-implant integration[9]. In regenerative medicine, it has been used to analyze regenerated bone structure[10,11].

Recently, microfocus X-ray CT has been used for 3D modeling of dental casts and applied to measure occlusal interaction[12]. Distances between upper and lower casts were compared before and after occlusal treatment. Also, by comparing dental cast models taken before and after occlusal adjustment of the tooth, the position and amount of adjustment were visualized[13].

The microfocus X-ray CT scanner has the advantage of capturing precise 3D shapes of deep fossa, and we propose a new method of measuring the three-dimensional morphology of a dental impression directly. This procedure omits one conversion process, impression to dental cast, and has the potential to improve accuracy. It has the advantage of reducing labor time, and moreover will solve a serious issue, the shortage of storage areas for dental casts at each treatment stage.

Microfocus X-ray CT has an intrinsic advantage because alternative methods, such as an optical scanner or contact probe, can not reach a complex concave surface. To the best of our knowledge, no reports have been published on the method of direct measurement and 3D modeling of rubber impressions. The aim of this study, therefore, was to evaluate the accuracy and precision of microfocus X-ray CT and to examine its applicability for direct three-dimensional impression modeling.

MATERIALS AND METHODS

Gage

To investigate the effect of the threshold value, two gages were used. Cross-section CT images have a gray scale value. To extract the surface of materials, the threshold value needs to be determined and usually an average value between the background and the material is used. The threshold value affects the size of the extracted surface[14], but not the pitch. Rectangular solids (Gage A) are used to measure width and steel balls (Gage B) to measure pitch.

An engineering plastic, Acetal Copolymer (Polyplastics Co. Ltd., Japan), was shaped into rectangular solids. Gage A comprised flat bars of three different sizes (4.00×8.00 mm, 12.00×16.00 mm, 20.00×24.00 mm in the XY plane and 8 mm in height) mounted on a plate (Fig. 1(a)). The width of Gage A was measured by a coordinate measuring machine, CMM (Crysta-Apex C9107; Mitsutoyo, Japan), and used as a reference.

Instead of using a machined surface, a 10 mm diameter steel ball bearing is a suitable standard gage because its sphericity is assured to less than 0.0007 mm (440C-G28; Tsubaki-Nakashima, Nara, Japan). Eight balls mounted on an aluminum plate and hemispherical surface were exposed (Fig. 2(a)). Ball center coordinates were measured by the same CMM and used to create STL models with CAD software.

Impression Materials

It is better for individual tray materials to have a lower X-ray absorption coefficient than that of impression materials. A metal tray is not suitable. Methyl methacrylate (MMA) resin (basing resin II; Quest Co., Aichi, Japan) was used for individual trays, and hydrophilic Vinyl Polysiloxane (EXAMIXFINE; GC Co., Tokyo, Japan) for impression materials. The material density of trays was smaller than that of the impression; the lower CT value of the tray helped to extract the impression surface. A tray was made specially for this experiment because there is no ready-made tray of suitable size for the standard gage. For precision, impression thickness is an issue and it is necessary to avoid a thin impression layer. The effect of tray space on accuracy was discussed in several cases[15]. Two sheets of paraffin wax were placed to control minimum impression thickness. Later it was verified as 2 mm on the CT cross-section image of the rubber impression.

Tray design also affects dimensional changes for impression[16,17]. Thickness uniformity of a tray and
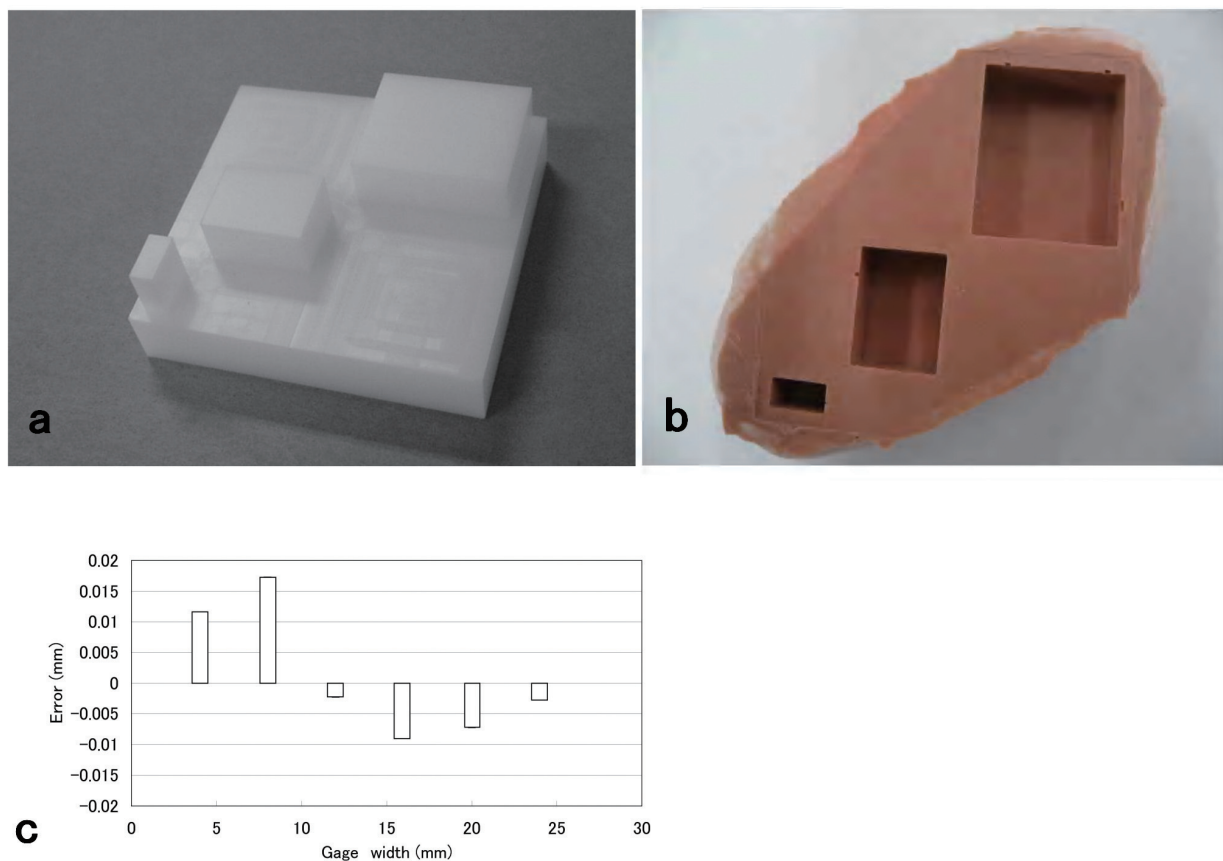

Fig. 1 (a) Gage A: flat bars of three different sizes mounted on a plate; (b) Rubber impression; (c) Relative error from CMM measurement.

overall strength is an issue to prevent deformation at removal. The impression was left to stand for at least 24 hours before pouring to avoid residual stress. Impressions of gage A and gage B are shown in (Fig. 1(b)) and (Fig. 2(b)).

Microfocus X-ray CT system
A microfocus X-ray CT system (SMX-225CT-SV; Shimadzu Corp., Japan) was used to construct 3D slice images. The maximum X-ray source output voltage, current, and minimum focus size were 225 kV, 1 mA, and 0.004 mm respectively. A 9-inch image intensifier with an aluminum window was used as an X-ray detector to convert X-ray fluoroscopic images into optical images, which were produced by a 1-mega pixel CCD camera. A sample was mounted on the rotating table with its axis perpendicular to the X-ray beam line. While the sample was rotated, multiple two-dimensional (2D) fluoroscopic images were acquired and sent to the computer to reconstruct 3D images. CT parameters were set and tuned to maximize image quality to produce a good polygonal model. The X-ray tube voltage and current used in this study were 170 kV and 0.09 mA, respectively. A total of 1200 fluoroscopic images were acquired with a total exposure time of 640 seconds. The reconstructed image size on the XY plane was 73.6 mm with a 1024×1024 matrix; therefore, each pixel was 0.072 mm.

On the cross-section image of gage A, the widths of the three flat bars (4, 8, 12, 16, 20, 24 mm) were measured. The threshold value was the average CT value between the air region and the rubber impression. Using a grayscale line profile crossing the sample edge, the actual edge was determined with accuracy less than the CT image matrix size.

3D models
To compare the 3D computer models, the STL (stereolithography) binary format was used. The STL file format is a polygon mesh and is a list of triangular surfaces that describes a computer-generated solid model. This file format is widely used in manufacturing and is a standard input for most rapid prototyping machines. CT images, which were layered, multiple-
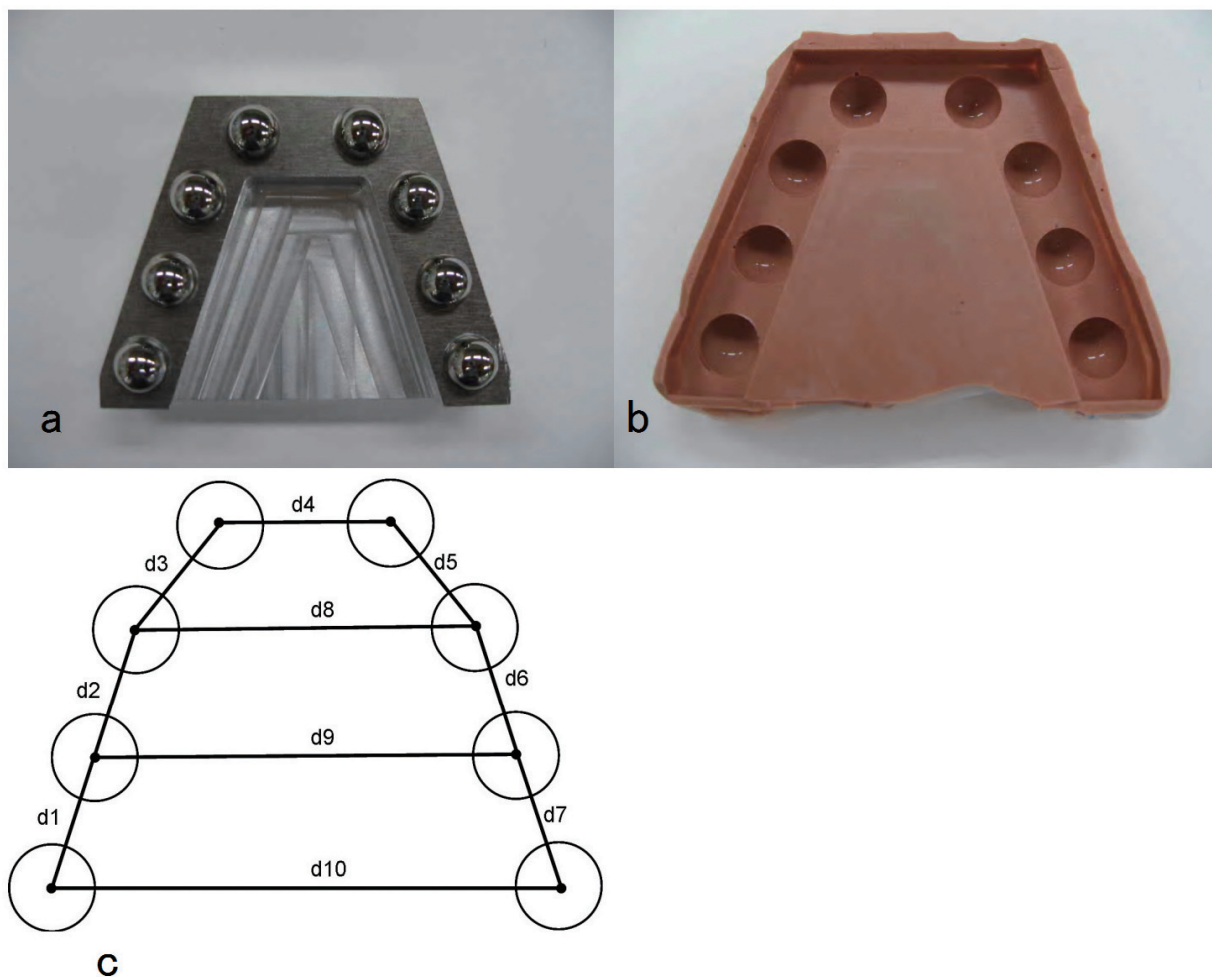

Fig. 2   (a) Gage B: Eight balls mounted on an aluminum plate; (b) Impression of eight balls; (c) Distances under evaluation.

sliced, cross-sectional images in 16-bit TIFF (Tagged Image File Format) format were converted into a STL 3D polygonal model using VG studio software (Volume Graphics GmbH, Heidelberg, Germany). To determine the relative density of the threshold which separated the internal and external regions, CT values of air and rubber impression portions were measured and their mean adopted as the threshold value. By choosing an appropriate X-ray tube voltage, 170 kV in this case, the effect of threshold variation in the object size can be minimized. Polygon mesh triangles in extraneous areas such as the base surface of the gage were deleted using Point Master software (Knotenpunkt GmbH, Germany). The STL model of the hemispherical surface of the eight balls had 18284 points and 35482 triangles. On the other hand, the STL model of CAD data of eight balls created with CMM data had 11664 points and 23296 triangles. For accurate and quantitative measurement of the two sets of computer models, superimposition was carried out using Point Master software to minimize the average distances between each pair of shells.

Evaluation measurement accuracy
Ball center distances are measured by a coordinate measuring function of VG studio software. By pointing the hemispherical surface on 3D images, the software calculates ball center coordinates. Two impressions were measured (No. 1, No. 2). The distances of each ball shown in Fig. 2 (c) were measured and compared with CMM data. The precision of the measuring system was defined as the standard deviation between two sets of 3D computer models of impressions measured in series in the same condition. For each polygon mesh lattice point of the reference polygon, the closest lattice point of the facing polygon was searched and the distance was measured using Point Master software. The minimum distance distribution was measured for statistical evaluation, then the distribution profile was exported and standard deviation was calculated.

impression were superimposed on the CAD model. Measurement accuracy was defined as the standard deviation between the impression and the CAD model.

Clinical application
This proposed method was applied in actual dental practice. Two individual trays were prepared to take an impression of the maxilla. One impression was scanned by microfocus CT and other was used to make a dental cast from hard gypsum (San-Esu Gypsum Co. Ltd., Hyogo, Japan), which was also scanned by CT and compared with the impression model.

RESULTS

Figure 1(c) shows the comparison of CT and CMM measurements using standard gages. Bar width had an error within ±0.02 mm, which was approximately one-quarter of the pixel size at 0.072 mm. The threshold level affects the bar widths. This error includes deformational changes of the impression, measurement errors of the CT scanner and the effect of the threshold level. Table 1 shows the measured distances of each ball center shown in Fig. 2 (c). The threshold level affects the ball diameter but does not affect ball center distances. This error includes deformational changes of the impression and measurement errors of the CT scanner. Error was less than 0.04 mm, larger than the error in Fig. 1(c), indicating that the effect of the threshold level was small compared to other factors. Average percent error of d1, d2, d3, d5, d6, d7 was 0.12%, equivalent to the accuracy, mainly depending on impression deformation, as reported in several papers[16,17,18].

Statistical evaluation was carried out using polygon mesh lattice point discordance. Figure 3 (a) shows the superimposition of two sets of 3D computer models of impressions measured in series in the same condition. Figure 3 (b) shows the distance distribution profile. This error value encompassed two aspects: microfocus CT system reproducibility and superimposition accuracy. Full width at half the maximum distribution was 0.033 mm, which was half of the pixel size. Standard deviation was less than 0.020 mm and measurement precision was evaluated as ±0.020 mm.

Figure 4 (a) shows the superimposition of two sets of 3D computer models of the impression and CAD model. Figure 4 (b) shows the distance distribution profile. Full width at half the maximum distribution is

Table 1   Distances of each ball center shown in Fig. 2

Label	d1	d2	d3	d4	d5	d6	d7	d8	d9	d10
CAD	15.80	15.81	15.61	20.00	15.62	15.81	15.81	40.00	50.00	60.00
No. 1 Error (mm)	0.026	0.019	0.018	−0.025	0.020	0.015	0.019	0.008	−0.008	0.029
No. 1 Error (%)	0.16	0.12	0.12	−0.13	0.13	0.10	0.12	0.02	−0.02	0.05
No. 2 Error (mm)	0.016	0.019	0.018	−0.025	0.010	0.025	0.019	−0.012	−0.028	0.039
No. 2 Error (%)	0.10	0.12	0.12	−0.13	0.06	0.16	0.12	−0.03	−0.06	0.06

Measured distances by CMM between each ball labeled in Fig. 2 (b), which is used as the CAD model. Two impressions were prepared (No. 1, No. 2), scanned by CT, and distances were measured. Errors of CMM measurements are shown.
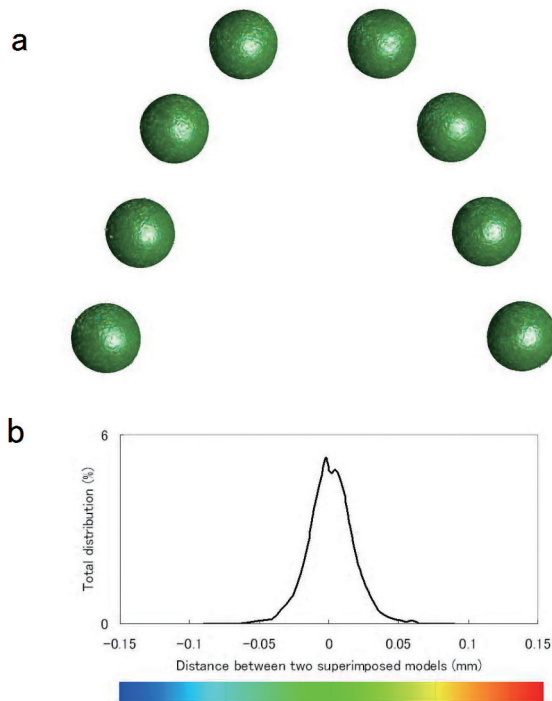
a

b

Fig. 3 (a) Superimposition of two computer models measured in series in the same condition by microfocus X-ray CT; (b) Color bar and distribution plot depend on the distance.
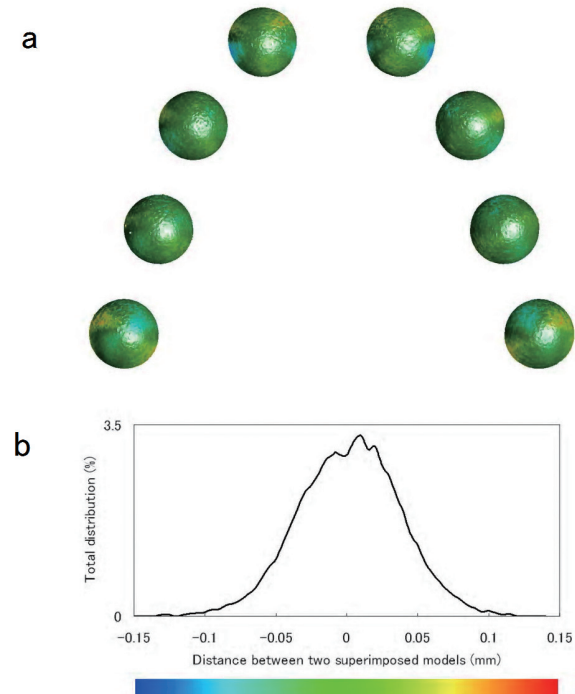
a

b

Fig. 4 (a) Contour map of 3D CT model in comparison to CAD model; (b) Color bar and distribution plot depend on the distance.

0.083 mm. Standard deviation was less than 0.050 mm and measurement accuracy was evaluated as ±0.050 mm.

The rubber impression model was compared with a stone cast model and is shown in Fig. 5. Both models were scanned by the same parameters and had the same voxel size. The area of the cervical margins is magnified in Figure 5 (b), (d). The rubber impression model had finer margins than the stone cast model.

DISCUSSION

The waiting time before pouring affects dimensional accuracy for stone[19]. Initially, we considered performing the CT scan immediately after impression extraction; however, in actual clinical application, the cost of microfocus CT is an issue and discourages installation in individual clinics. We assumed that an impression would be delivered to a dental lab by a door-to-door delivery service. In this report, measurements were made 24–48 hours after making the impression. This report showed that deformation was small enough for application, even though the impression was kept for more than 24 hours.

With the recent development of parallel computing, CT reconstruction time has fallen markedly and so called high performance computing (HPC) technology

has made it possible to complete reconstruction within 5 sec after finishing data acquisition. Even though microfocus CT is mostly used in research laboratories at the moment, it will gain popularity in the clinical field with further cost-cutting efforts.

Precision and accuracy, as shown in Figures 2 and 3, were smaller than the CT pixel size, which was determined by the field of view size and reconstruction matrix. This result was attributed to the characteristics of the CT scanner. Output data from an optical scanner or probe scanner were in the form of a 3D point cloud. To improve the accuracy of the optical scanner, the number of sampling points needed to be increased. On the other hand, the CT scanner produced grayscale slice images. Each pixel had a grayscale value and was separated into internal and external regions by the relative density of the threshold. Polygon mesh lattice points were located between two neighboring pixels, in which one pixel was in the internal and the other was in the external region. By proportional division of the relative CT value of the threshold, lattice points were determined in sub-pixel resolution. Therefore, it was important to maximize not only spatial resolution, but also the signal-to-noise ratio (SN) of images. Using a grayscale line profile crossing the sample edge, it was possible to achieve accuracy smaller than the pixel size.
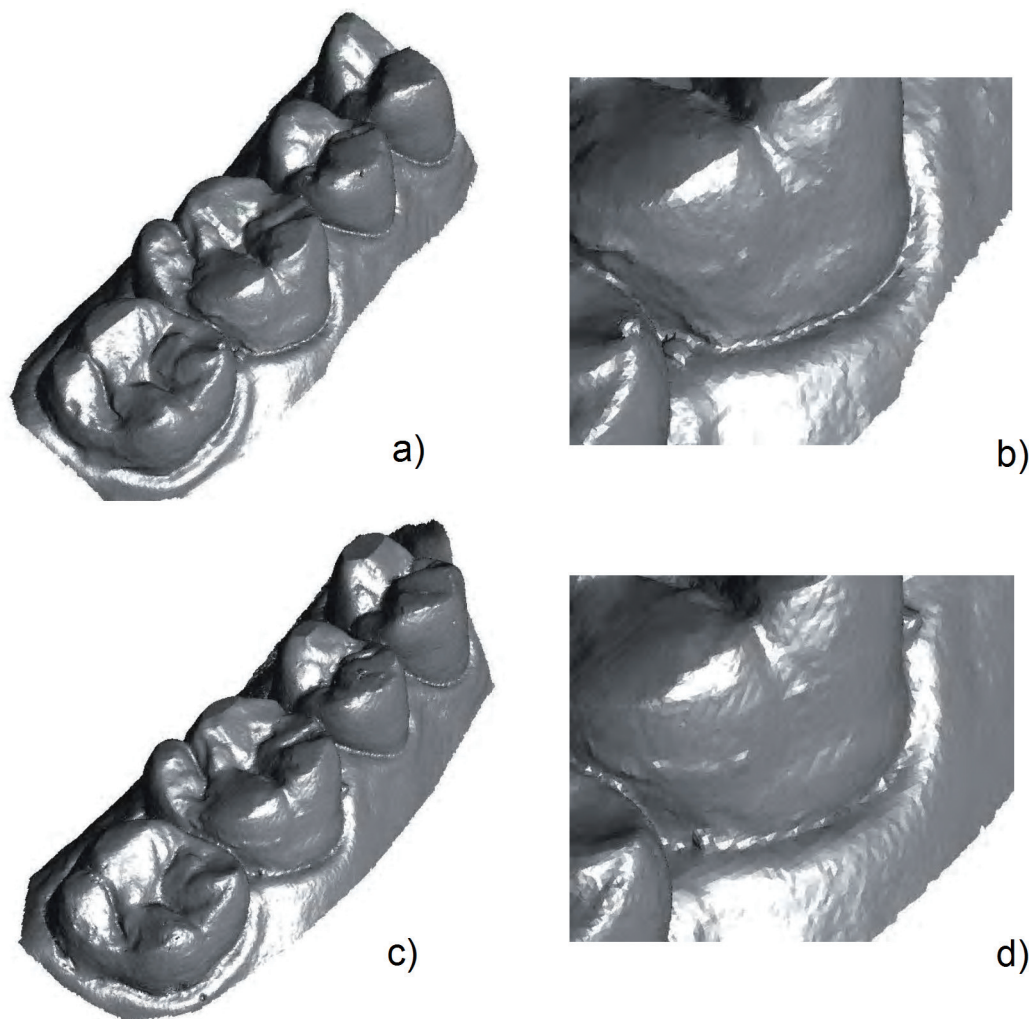
Fig. 5 (a) Rubber impression model of maxilla; (b) Magnified image of (a), first molar; (c) Cast model; (d) Magnified image of (c), first molar.

At this juncture, it is worth noting that creating a 3D computer model from grayscale data was a process that converted grayscale values into spatial information, which was different from simple spatial interpolation of point group data. Both spatial resolution and SN are factors that affect system accuracy. Spatial resolution was determined by the pixel size of the detector, view (fluoroscopic image) number, and CT reconstruction matrix. SN was determined by the total exposure time, X-ray dose, and X-ray voltage. A longer exposure time and a higher X-ray dose would provide a better SN. Depending on the sample size and material (silicon rubber in this case), optimum X-ray voltage could be achieved.

In this report, we used two different methods to examine accuracy: one used distinguishing dimensional features, such as ball center distances and the other compared each polygon mesh lattice point. The former features represent average points of a related polygon

and the results tend to be better than in the latter method. It is important to discuss accuracy in both respects. Results are shown on a color difference map in Fig. 3 and errors are almost equivalent to 3D evaluation by a laser scanner[5]. Errors include two factors, impression accuracy and measurement accuracy.

By comparing cervical margins of the rubber impression model with the stone cast model in Fig. 4, the results indicate the significance of the proposed method. The conversion process of making the cast diminishes fine features in general. When the original stone cast was observed and compared with the CT model, the cast had finer margins than the computer model. It is considered that the inherent character of microfocus CT contributes to diminish fine features, especially with concave surfaces. Cross-section images are constructed using many views from 360 degrees. A longer penetration pass causes X-ray scattering and

increases image noise. Comparing two different shapes, concavity and convexity, 360-degree transmitted images around convex features have less penetration pass than that around concave features. The cervical margin of the rubber impression is convex and the cervical margin of the cast is concave; therefore, scanning a rubber impression is suitable to preserve the fine morphology of the cervical margin.

As we discussed above, the findings of this study revealed that microfocus X-ray CT offered a practical method to construct 3D computer models of impressions.

CONCLUSIONS

Within the limitations of this study, microfocus X-ray CT indicated that the accuracy is sufficient to serve as an input device for direct three-dimensional modeling of silicone rubber impressions.

REFERENCES

1) Sohmura T, Kojima T, Wakabayashi K, Takahashi J. Use of an ultrahigh-speed laser scanner for constructing three-dimensional shapes of dentition and occlusion. J Prosthet Dent 2000; 84: 345-352.
2) DeLong R, Heinzen M, Hodges JS, Ko CC, Douglas WH. Accuracy of a system for creating 3D computer models of dental arches. J Dent Res 2003; 82: 438-442.
3) Brosky ME, Major RJ, DeLong R, Hodges JS. Evaluation of dental arch reproduction using three-dimensional optical digitization. J Prosthet Dent 2003; 90: 434-440.
4) Olthoff LW, van der Zel JM, de Ruiter WJ, Vlaar ST, Bosman F. Computer modeling of occlusal surfaces of posterior teeth with the CICERO CAD/CAM system. J Prosthet Dent 2000; 84: 154-162.
5) Persson A, Andersson M, Oden A, Sandborgh-Englund G. A three-dimensional evaluation of a laser scanner and a touch-probe scanner. J Prosthet Dent 2006; 95: 194-200.
6) Hirakimoto A, Ohnishi S, Maeda H, Kishi T, Shiota T, Tamura T, Ukita M. Fujita S. Kamegawa M. Progress of microfocus X-ray systems for fluoroscopic and computed tomography. Spectrochimica Acta Part B 2004; 59: 1101-1106.
7) Bergmans L, Cleynenbreugel JV, Wevers M, Lambrechts P. A methodology for quantitative evaluation of root canal instrumentation using microcomputed tomography. International Endodontic J 2001; 34: 390-398.
8) Wakabayashi K, Sohmura T, Nakamura T, Kojima T, Kinuta S, Takahashi J, Yatani H. New evaluation method by microfocus radiograph CT for 3D assessment of internal adaptation of all-ceramic crowns. Dent Mater J 2005; 24: 362-367.
9) Butz F, Ogawa T, Chang T, Nishimura I. Three-dimensional bone-implant integration profiling using micro-computed tomography. Int J Oral Maxillofac Implants 2006; 21: 687-695.
10) Rai B, Ho K, Lei Y, Si-Hoe K, Teo C, Yacob K, *et al.* Polycaprolactone-20% tricalcium phosphate scaffolds in combination with platelet-rich plasma for the treatment of critical-sized defects of the mandible: a pilot study. J Oral Maxillofac Surg 2007; 65: 2195-2205.
11) Kinoshita Y, Matsuo M, Todoki K, Ozono S, Fukuda S, Tsuzuki H, Nakamura M, Tomihata K, Shimamoto T, Ikada Y. Alveolar bone regeneration using absorbable poly beta-tricalcium phosphate membrane and gelatin sponge incorporating basic fibroblast growth factor. Int J Oral Maxillofac Surg 2008; 37: 275-281.
12) Kamegawa M, Nakamura M, Tsutsumi S. 3D Morphological Measurements of Dental Casts with Occlusal Relationship using Microfocus X-ray CT. Dent Mater J 2008; 27: 549-554.
13) Kamegawa M, Nakamura M, Kitahara K, Ohtomo H, Hasegawa T, Nakakura T, Tsutsumi S. 3-D morphological assessment of occlusal treatment by measuring dental casts with a micro-focus X-ray CT. J Oral Rehabil 2008; 35: 382-389.
14) Sohmura T, Wakabayashi K, Lowmunkong R, Hojo H, Kusumoto N, Okuda H, Kojima T, Nakamura T, Yatani H, Takahashi J. 3D shape measurement of dental casts using medical X-ray CT. Dent Mater J 2004; 23: 121-128.
15) Tjan AHL, Nemetz H, Nguyen LTP, Contino R. Effect of tray space on the accuracy of monophasic polyvinylsiloxane impressions. J Prosthet Dent 1992; 64: 19-28.
16) Gordon GE, Johnson GH, Drennon DG. The effect of tray selection on the accuracy of elastomeric impression materials. J Prosthet Dent 1990; 68: 12-15.
17) Boulton JL, Gage JP, Vincent PF, Basford KE. A laboratory study of dimensional changes for three elastomeric impression materials using custom and stock trays. Australian Dent J 1996; 41: 398-404.
18) Johnson GH, Craig RG. Accuracy of four types of rubber impression materials compared with time of pour and a repeat pour of models. J Prosthet Dent 1985; 53: 484-490.
19) Lacy AM, Bellman T, Fukui H, Jendresen MD. Time-dependent accuracy of elastomer impression materials. Part I: Condensation silicones. J Prosthet Dent 1981; 45: 209-215.